



Biophysical effects on the interannual variation in carbon dioxide exchange of an alpine meadow on the Tibetan Plateau

Lei Wang¹, Huizhi Liu¹, Jihua Sun^{2,3}, and Yaping Shao³

¹LAPC, Institute of Atmospheric Physics, Chinese Academy of Sciences, Beijing 100029, China

²Meteorological Observatory of Yunnan Province, Kunming 650034, China

³Institute for Geophysics and Meteorology, University of Cologne, Cologne, 50937, Germany

Correspondence to: Huizhi Liu (huizhil@mail.iap.ac.cn)

Received: 29 November 2016 – Discussion started: 23 December 2016

Revised: 17 March 2017 – Accepted: 27 March 2017 – Published: 20 April 2017

Abstract. Eddy covariance measurements from 2012 to 2015 were used to investigate the interannual variation in carbon dioxide exchange and its control over an alpine meadow on the south-east margin of the Tibetan Plateau. The annual net ecosystem exchange (NEE) in the 4 years from 2012 to 2015 was -114.2 , -158.5 , -159.9 and -212.6 g C m⁻² yr⁻¹, and generally decreased with the mean annual air temperature (MAT). An exception occurred in 2014, which had the highest MAT. This was attributed to higher ecosystem respiration (RE) and similar gross primary production (GPP) in 2014 because the GPP increased with the MAT, but became saturated due to the limit in photosynthetic capacity. In the spring (March to May) of 2012, low air temperature (T_a) and drought events delayed grass germination and reduced GPP. In the late wet season (September to October) of 2012 and 2013, the low T_a in September and its negative effects on vegetation growth caused earlier grass senescence and significantly lower GPP. This indicates that the seasonal pattern of T_a has a substantial effect on the annual total GPP, which is consistent with results obtained using the homogeneity-of-slopes (HOS) model. The model results showed that the climatic seasonal variation explained 48.6 % of the GPP variability, while the percentages explained by climatic interannual variation and the ecosystem functional change were 9.7 and 10.6 %, respectively.

1 Introduction

In the last decade, the carbon dioxide exchange in grassland ecosystems has attracted much attention (Baldocchi, 2008; Huang et al., 2008; Hunt et al., 2004; Jing et al., 2010; Suyker et al., 2003) because grasslands cover 32 % of the global land surface and make a substantial contribution to the carbon cycle on a global scale (Parton et al., 1995). The annual net ecosystem exchange (NEE) of grasslands has a large range, from -650 to 160 g C m⁻² yr⁻¹, due to climate variability and land use changes (Gilmanov et al., 2007; Wang et al., 2016a). The climatic factors controlling CO₂ exchange also vary under different climate conditions (Du and Liu, 2013; Huang et al., 2016; Xu and Baldocchi, 2004). Most previous studies have focused on low-lying grasslands (Gilmanov et al., 2010).

Alpine meadows in China are the primary grassland type of the nation and are mainly distributed in the Qinghai-Tibetan plateau (DAHV and CISNR, 1996; Liu et al., 2008). The warming trend in high-altitude areas, such as the Tibetan Plateau and its south-east margin, has been observed to be more pronounced (Fan et al., 2011; Liu and Chen, 2000). Several studies of CO₂ exchange have been carried out on the Qinghai-Tibetan plateau, where the mean annual air temperature (T_a) is approximately 0 °C (Gu et al., 2003; Kato et al., 2006; Shi et al., 2006; Zhao et al., 2006). The daily CO₂ fluxes of the alpine meadow steppe in Damxung, Tibet were shown to be jointly affected by T_a and soil moisture (Fu et al., 2009), while the daily CO₂ fluxes of an alpine shrubland at Haibei, Qinghai were found to be sensitive to T_a (Zhao et al., 2006). On an annual scale, the measurements at the Haibei

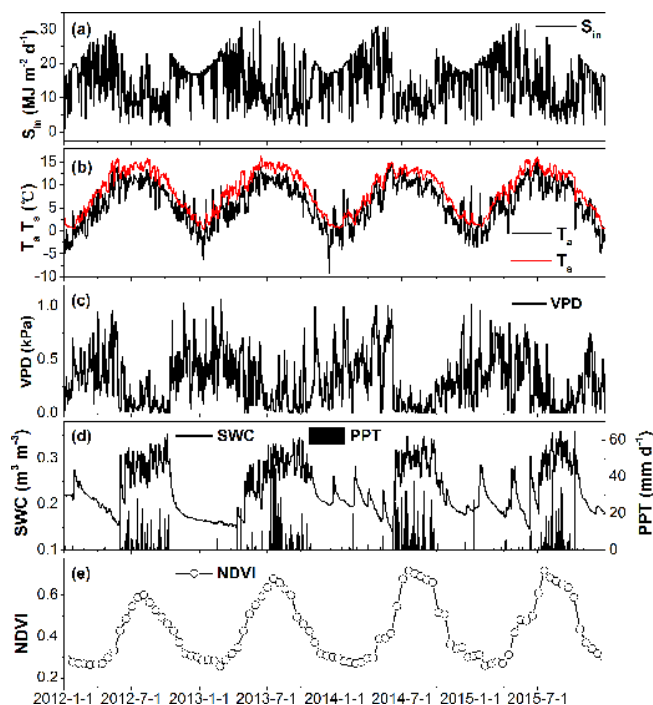


Figure 1. (a) Daily sum of solar radiation (S_{in}), (b) daily mean air temperature (T_a), soil temperature (T_s), (c) vapour pressure deficit (VPD, 5 cm), (d) soil water content (SWC, 5 cm), daily total precipitation (PPT) and (e) 16-day average normalized difference vegetation index (NDVI) from 2012 to 2015.

alpine meadow revealed that the annual CO_2 uptake was increased by the earlier onset of the growing season, which was caused by higher T_a (Kato et al., 2006). The Lijiang alpine meadow is located in a much warmer area (the mean annual T_a is 12.7°C). A spring drought event and relatively low soil moisture were shown to significantly delay the start time of grass germination and reduce the annual CO_2 uptake (Wang et al., 2016b). How the annual CO_2 exchange responds to the mean annual T_a is not clear for alpine meadow ecosystems.

Previous studies have attributed year-to-year changes in CO_2 exchange to climatic variability (Hui et al., 2003; Xu and Baldocchi, 2004). Fluxes may directly respond to climatic drivers or be indirectly affected by functional changes or changes in the flux–climate relationships (Polley et al., 2008). Statistical models have been used to partition the interannual variation (IAV) of the CO_2 exchange (Hui et al., 2003; Richardson et al., 2007; Teklemariam et al., 2010). For example, Shao et al. (2014) found that 77 % of the observed variation in NEE was explained by functional changes in the moist grassland in USA, while variations in climatic variables could better explain the IAV of NEE of a meadow in Denmark (Jensen et al., 2017) and mixed-grass prairies in the semi-arid area of USA (Polley et al., 2008). The relative importance of the direct and indirect effects of the climatic

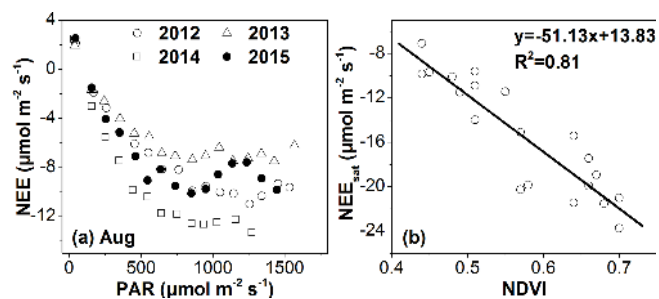


Figure 2. The relationship between daytime NEE and PAR (a) for August from 2012 to 2015. The NEE and PAR data were averaged with PAR bins of $100 \mu\text{mol m}^{-2} \text{s}^{-1}$. (b) The relationship between NEE_{sat} and NDVI on a monthly scale.

variables on the interannual variations in CO_2 exchange for alpine meadows in China has not been quantified.

The CO_2 exchange between the atmosphere and the Lijiang alpine meadow was measured using an eddy covariance technique from 2012 to 2015. The objectives of this study were to (1) examine the seasonal and interannual variation in NEE, gross primary production (GPP), ecosystem respiration (RE) and the parameters of ecosystem photosynthesis and RE; (2) investigate the main environmental controls of the total GPP, RE and NEE on seasonal and annual scales; and (3) partition the interannual variation in GPP, RE and NEE into climatic variability and vegetation growth.

2 Observation site and methods

2.1 Observation site

The observation site ($27^\circ 10' \text{N}$, $100^\circ 14' \text{E}$, 3560 m a.s.l.) is located at Maoniuping in the Yulong snow mountains, to the north of Lijiang city on the south-east margin of the Tibetan Plateau, China. The study area has a plateau monsoon climate, which is influenced by the south-west and south-east monsoons. There are distinct wet and dry seasons, with a wet season from June to October. The 30-year mean annual total precipitation (1981–2010) at Lijiang city (2400 m a.s.l.) is 980.3 mm, and 85 % of the precipitation is concentrated in the wet season. The 30-year mean annual air temperature (MAT) is 12.6°C (data from the Lijiang Meteorology Bureau). The dominant species in this alpine meadow are grass of the genus *Kobresia Willd.*, with a maximum height of 20 cm, and the shrub *Berberis Linn.*, with a maximum height of more than 60 cm. The surface is covered by green vegetation, litter and bare soil. The soil type is a loam, with a dark brown colour, which has a lower reflectance than the grass canopy (Guo et al., 2009).

Table 1. The average value of daily solar radiation (S_{in} , $\text{MJ m}^{-2} \text{d}^{-1}$), the mean annual air temperature (T_a , $^{\circ}\text{C}$), the mean annual vapour pressure deficit (VPD, kPa), the mean annual soil water content (SWC, $\text{m}^3 \text{m}^{-3}$), the total amount of precipitation (PPT, mm) for the whole year and the wet season, and the maximum value of NDVI for each year from 2011 to 2015.

Variables	2012	2013	2014	2015
S_{in}	14.23	14.40	14.44	14.59
T_a	5.93	5.92	6.32	6.16
VPD	0.32	0.30	0.32	0.30
SWC	0.232	0.227	0.232	0.233
PPT (whole year)	1190.4	1066.1	1204.8	1257.4
PPT (wet season)	1086.5	906.1	1092.6	1067.1
NDVI_{\max}	0.60	0.68	0.72	0.72

2.2 Field measurements and normalized difference vegetation index (NDVI)

The eddy covariance (EC) system was used to measure 3-D wind speed and the H_2O and CO_2 concentrations at a height of 2.5 m, with a 10 Hz frequency. The system consisted of a three-dimensional sonic anemometer (CSAT3, Campbell Scientific, Logan, UT, USA) and an open-path $\text{CO}_2/\text{H}_2\text{O}$ infrared gas analyzer (LI-7500A, LI-COR, Lincoln, NE, USA). The low response measurements (1/3 Hz frequency) made in this study were T_a and relative humidity at a height of 2.5 m close to the EC system (HMP45C, Campbell Scientific). Net radiation (including shortwave and longwave radiation, CNR4, Kipp&Zonen, Delft, Netherlands) and photosynthetically active radiation (PAR; LI190SB, LI-COR) were measured at 1.5 m. Soil temperature (109-L, Campbell Scientific) and soil water content (SWC; CS616, Campbell Scientific) were measured at a depth of 5 cm below the ground. The precipitation (including solid precipitation in the winter) was measured using a weighing bucket precipitation gauge (T-200B, Geonor, Eiksmarka, Norway). All measurements were controlled by a data logger (CR3000, Campbell Scientific), and the data were stored on a 2-GB CF card.

Four points around the flux tower were selected to investigate the variations in vegetation growth. The $250 \times 250 \text{ m}^2$ gridded NDVI data at 16-day intervals (product name: MOD13Q1) for the four points were obtained from the Moderate Resolution Imaging Spectrometer (MODIS) on the EOS-1Terra satellite and were averaged to represent the meadow at this observation site. Observations affected by clouds were removed during this process, and the gaps were filled linearly.

2.3 Flux calculation and quality control

EddyPro software (version 5.1, LI-COR) was used to calculate the half-hourly CO_2 flux based on the 10 Hz raw data. After a spike detection (Vickers and Mahrt, 1997), the sector-

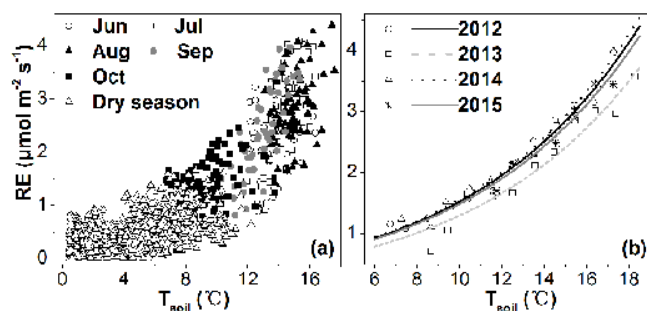


Figure 3. (a) Relationship between RE and T_{soil} in 2012; (b) relationship between RE and T_{soil} for the wet season from 2012 to 2015; RE and T_{soil} were averaged with T_{soil} bins of 1°C .

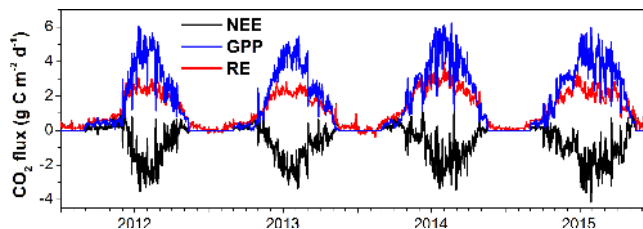


Figure 4. The daily mean NEE, GPP and RE from 2012 to 2015.

wise planar fit method was used to transform the coordinate system due to a terrain slope of approximately 10° (Wilczak et al., 2001). The CO_2 flux was also subjected to a spectral loss correction (Moore, 1986) and density correction (WPL correction; Webb et al., 1980).

Stationary and integral turbulence characteristics tests were used for flux quality control (Foken and Wichura, 1996). When u^* was less than 0.1 m s^{-1} , the CO_2 flux was dependent on u^* and was discarded. Because there was a coniferous forest approximately 350 m to the north of the site, an analytical footprint model was used to determine whether the half-hourly CO_2 flux was influenced by the forest and needed to be removed (Kormann and Meixner, 2001).

After quality control, approximately 70 % of the CO_2 fluxes were subjected to further analysis. Linear interpolation was used to fill flux gaps of less than 2 h. To fill gaps of longer than 2 h, marginal distribution sampling, an improved look-up table method, was used (Falge et al., 2001; Lloyd and Taylor, 1994).

2.4 Data analysis

Using the homogeneity-of-slopes (HOS) model (Hui et al., 2003), the control of the CO_2 exchanges (NEE, GPP and RE) was statistically partitioned into four components: the inter-annual variation of environmental variables (SS_i), the seasonal variation of environmental variables (SS_s), variations of biological variables (SS_f , NDVI in this study) and random error (SS_e , resulting from measurement and analysis random error). To identify the significant control variables, a multi-

Table 2. The ecosystem photosynthesis parameters using Eq. (1) (NEE_{sat} : $\mu\text{mol m}^{-2} \text{s}^{-1}$, α : $\mu\text{mol m}^{-2} \text{s}^{-1}$, R^2) and NDVI for each month during the wet seasons from 2012 to 2015. The regression was based on the average values of NEE_{daytime} and PAR with PAR bins of $100 \mu\text{mol m}^{-2} \text{s}^{-1}$. $NEE_{\text{sat}}^{(a)}$ represents the mean value and the standard deviation, $NEE_{\text{sat}}^{(b)}$ and $NEE_{\text{sat}}^{(c)}$ represent the maximum and minimum values of NEE_{sat} for each month.

Month	NEE_{sat}^a	NEE_{sat}^b	NEE_{sat}^c	α	RE_{bulk}
June	-11.59 ± 2.45	-9.69	-15.08	-0.037 ± 0.009	3.59 ± 0.52
July	-19.67 ± 1.54	-17.46	-21	-0.050 ± 0.009	3.75 ± 0.83
August	-20.14 ± 3.52	-15.43	-23.75	-0.055 ± 0.016	4.15 ± 0.74
September	-16.44 ± 4.56	-11.43	-21.44	-0.051 ± 0.017	3.70 ± 1.04
October	-9.36 ± 1.62	-7.08	-10.9	-0.031 ± 0.005	2.45 ± 0.37

ple stepwise regression analysis of the CO_2 exchanges with environmental variables was conducted using SPSS 12.0 for Windows (SPSS Inc., Chicago, IL, USA). The environmental variables that were significantly correlated with fluxes were submitted for further HOS analysis, while the others were excluded from the analysis. To minimize errors, the daily NEE, GPP and RE were excluded from regressions if more than 50 % of the data points in the daytime ($R_n > 5 \text{ W m}^{-2}$) were missing. More details of the HOS model are provided in Hui et al. (2003).

The relationship between daytime NEE (NEE_{daytime}) and PAR was described by the Michaelis–Menten model (Falge et al., 2001):

$$NEE_{\text{daytime}} = \frac{\alpha NEE_{\text{sat}} \text{PAR}}{\alpha \text{PAR} + NEE_{\text{sat}}} + RE_{\text{bulk}}, \quad (1)$$

where NEE_{sat} is the NEE at the saturated light level, α is the apparent quantum yield ($\mu\text{mol CO}_2 \mu\text{mol}^{-1}$ photons), and RE_{bulk} is the bulk estimated RE.

The Van 't Hoff equation was used to evaluate the relationship between the night-time NEE ($NEE_{\text{nighttime}}$, $\mu\text{mol CO}_2 \text{m}^{-2} \text{s}^{-1}$) and soil temperature at a depth of 5 cm (T_s , °C; Aires et al., 2008):

$$NEE_{\text{nighttime}} = a \exp(bT_s), \quad (2)$$

where a and b are the regression parameters. The temperature sensitivity coefficient (Q_{10}) of RE was determined using the following equation.

$$Q_{10} = \exp(10b) \quad (3)$$

The partitioning of NEE into GPP and RE was based on the assumption that the sensitivity of RE to soil temperature was the same during the day and at night (Falge et al., 2001). The regression parameters derived from the night-time data were extrapolated to the daytime to calculate the daytime RE and the daily RE. The daily GPP was calculated as follows:

$$\text{GPP} = \text{RE} - \text{NEE}. \quad (4)$$

3 Results

3.1 Weather conditions and NDVI

The daily integrated solar radiation (S_{in}) varied from 1.15 to $32.40 \text{ MJ m}^{-2} \text{d}^{-1}$ (Fig. 1a). The mean S_{in} in spring (March to May) was 17.0 to $19.93 \text{ MJ m}^{-2} \text{d}^{-1}$ and was clearly larger than in other seasons. In the wet season, the mean S_{in} was 9.99 to $11.05 \text{ MJ m}^{-2} \text{d}^{-1}$.

The MAT was 5.92 to 6.32 °C (Table 1). The daily mean T_a ranged from 0.41 to 14.96 °C in the wet season and decreased to a minimum value of -9.06 °C in the winter. In contrast, the soil temperature never decreased below 0 °C, and the maximum value was 16.48 °C (Fig. 1b). The vapour pressure deficit (VPD) reached its maximum value of 1.07 kPa before the wet season (Fig. 1c). The VPD decreased to near 0 kPa, and the mean VPD for the wet season was 0.125 to 0.166 kPa.

The annual precipitation from 2012 to 2015 ranged from 1066.1 to 1257.4 mm. The precipitation during the wet season ranged from 906.1 to 1092.6 mm, accounting for 85 to 91 % of the annual total precipitation (Table 1). The mean annual SWC had a small interannual variability, from 0.227 to $0.233 \text{ m}^3 \text{m}^{-3}$. In the wet season, the SWC reached a maximum value of approximately $0.35 \text{ m}^3 \text{m}^{-3}$, and the minimum SWC was $0.15 \text{ m}^3 \text{m}^{-3}$ (Fig. 1d).

The NDVI of this alpine meadow displayed a clear seasonal and interannual variation (Fig. 1e). The NDVI exceeded 0.4 at the end of April or in late May, depending on the amount and distribution of precipitation in the spring (March to May). The maximum NDVI for each year ranged from 0.60 (2012) to 0.72 (2013). In all 4 years, the NDVI decreased to below 0.4 at the end of October.

3.2 Seasonal and interannual variations in NEE_{sat} , α and Q_{10}

The daytime NEE and PAR were averaged, with PAR bins of $100 \mu\text{mol m}^{-2} \text{s}^{-1}$ to avoid random errors. For each month in the wet season, the daytime NEE decreased with PAR until a critical PAR was reached. Above the critical PAR, the daytime NEE increased and the CO_2 uptake was de-

Table 3. The ecosystem respiration parameters using Eqs. (2) and (3) (a: $\mu\text{mol m}^{-2} \text{s}^{-1}$, b: Q_{10} , R^2) for the wet and dry seasons from 2012 to 2015. The regression was based on the average values of RE and T_{soil} with T_{soil} bins of 1°C .

Season	Year	a	b	Q_{10}	R^2
Wet season	2012	0.437	0.125	3.48	0.98
	2013	0.374	0.124	3.46	0.94
	2014	0.442	0.126	3.51	0.98
	2015	0.433	0.123	3.43	0.98
Dry season	2012	0.338	0.081	2.25	0.78
	2013	0.202	0.096	2.60	0.74
	2014	0.283	0.115	3.15	0.99
	2015	0.313	0.104	2.82	0.70

pressed (Fig. 2a). To derive NEE_{sat} and α , the NEE and PAR data were used only when PAR was below the critical value. NEE_{sat} showed a clear seasonal variation (Table 2). The mean NEE_{sat} values for each month showed that NEE_{sat} began to increase in June ($-11.59 \mu\text{mol m}^{-2} \text{s}^{-1}$) and reached a maximum in August ($-20.14 \mu\text{mol m}^{-2} \text{s}^{-1}$). The highest NEE_{sat} during the whole observation period occurred in August of 2014 ($-23.75 \mu\text{mol m}^{-2} \text{s}^{-1}$). NEE_{sat} then declined with grass senescence in September and October. The NEE_{sat} in October ($-9.36 \mu\text{mol m}^{-2} \text{s}^{-1}$) was less than half that in August. The interannual variations in NEE_{sat} were also large. For example, NEE_{sat} in September 2015 ($-21.44 \mu\text{mol m}^{-2} \text{s}^{-1}$) was almost twice that in September 2013 ($-11.43 \mu\text{mol m}^{-2} \text{s}^{-1}$; Table 2). On a monthly scale, 81 % of the variation in NEE_{sat} could be explained by the mean NDVI (Fig. 2b). Over this meadow, NEE_{sat} did not significantly correlate with SWC because the soil water conditions were always good in the wet season.

At monthly intervals, there were large random errors in the regression between RE and T_{soil} . For example, the R^2 for each month of the wet season in 2012 ranged from 0.04 to 0.12. Thus, in 2012, the data in the wet and dry season were combined to fit the regression (Fig. 3a). The Q_{10} in the wet seasons was similar, at approximately 3.45 (Table 3), which was in the normal range of previous studies (1.2 to 3.7; Falge et al., 2001). These values were clearly higher than those for temperate grasslands (1.99 to 3.07; Wang et al., 2016a), Mediterranean grasslands (1.22 to 2.36; Aires et al., 2008) and the Haibei alpine meadow (1.50 to 2.27; Kato et al., 2004). Q_{10} was lower in the dry season than in the wet season.

3.3 Seasonal and interannual variation in NEE, GPP and RE

The ecosystem started to absorb CO_2 (negative value of NEE) on DOY 165 in 2012, DOY 137 in 2013, DOY 116 in 2014 and DOY 104 in 2015, and then NEE decreased (Fig. 4). The minimum daily NEE for each year occurred

Table 4. The annual total NEE, GPP and RE ($\text{g C m}^{-2} \text{yr}^{-1}$) for each year from 2012 to 2015.

	2012	2013	2014	2015
NEE	-114.2	-158.5	-159.9	-212.6
GPP	522.3	546.5	669.4	661.8
RE	412.1	393.6	515.2	456.7

Table 5. The percentage of the contributions of the seasonal climatic variation (SS_s), interannual climatic variability (SS_i), the ecosystem functional change (SS_f) and random error (SS_e) to the interannual variations in NEE, GPP and RE.

	SS_s	SS_i	SS_f	SS_e
NEE	37.7 %	7.7 %	10.3 %	44.3 %
GPP	48.6 %	9.7 %	10.7 %	31.0 %
RE	48.6 %	15.6 %	21.2 %	14.6 %

in July or August (-3.52 on DOY 196 in 2012, -3.35 on DOY 218 in 2013, -3.43 on DOY 243 in 2014 and $-4.16 \text{g C m}^{-2} \text{d}^{-1}$ on DOY 210 in 2015). NEE increased significantly in September and became positive on DOY 293 in 2012, DOY 305 in 2013, DOY 295 in 2014 and DOY 297 in 2015. The maximum difference in the start time of CO_2 uptake was 61 days while the difference in the end time was 12 days. The CO_2 uptake period was much shorter in 2012 (129 days) than in 2013 (169 days), 2014 (180 days) and 2015 (194 days).

The daily GPP increase started earlier than CO_2 uptake. The seasonal pattern of daily GPP was similar to that of NEE, although the amplitude of GPP variations was larger than that of NEE variations. The maximum daily GPP for each year was 6.02, 5.47, 6.23 and $5.95 \text{g C m}^{-2} \text{d}^{-1}$ for the 4 years from 2012 to 2015. Compared with the NEE and GPP, the seasonal variation in RE was smaller during the wet season. In particular, RE varied only slightly from June to August.

The annual GPP in 2014 and 2015 was clearly higher than in 2012 and 2013, as indicated by the larger NDVI (Fig. 5; Tables 1, 4). In contrast, the RE in 2014 was the highest of all 4 years because, although the Q_{10} value was similar to the other years, it had the highest T_a (Table 1). Therefore, the annual NEE in 2014 was similar to that in 2013, but lower than that in 2015, although the GPP was similar in 2014 and 2015. The spring drought resulted in a significantly lower NDVI in 2012 than in the other years; consequently, the annual GPP in 2012 was the lowest of all 4 years. The annual NEE for the 4 years followed the order of $2015 < 2014 < 2013 < 2012$ (Table 4), which is consistent with the length of the CO_2 uptake period.

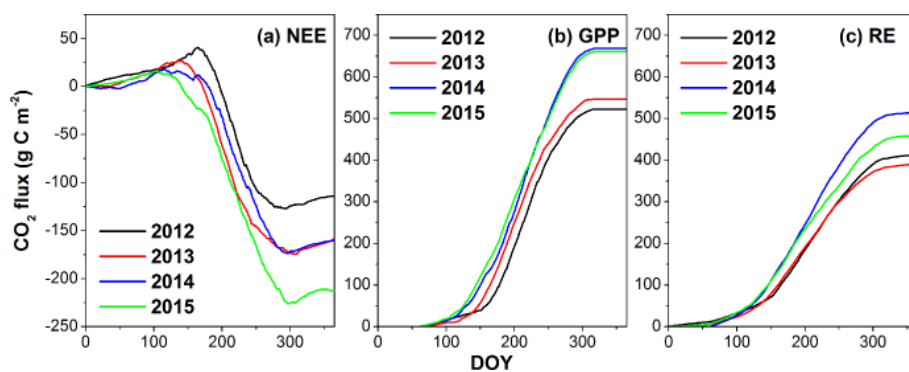


Figure 5. The cumulative NEE, GPP and RE from 2012 to 2015.

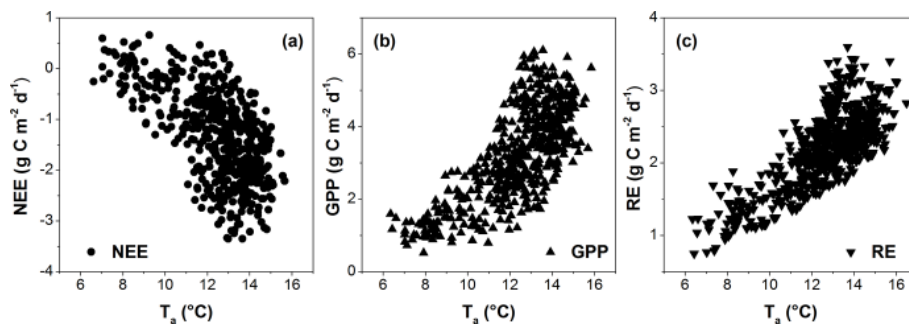


Figure 6. Relationships between (a) NEE and T_a , (b) GPP and T_a and (c) RE and T_a for the wet seasons from 2012 to 2015.

Table 6. The GPP_{diff} for 2013–2012, 2014–2012 and 2015–2012 during the periods from March to May, June, from June to July and from August to September.

Periods	GPP_{diff}		
	2013–2012	2014–2012	2015–2012
March to May	20.0	63.1 (43 %)	83.3 (60 %)
June	28.7	13.4 (9 %)	23.7 (17 %)
July to August	−8.7	14.2 (10 %)	−18.5 (−13 %)
September to October	−12.0	55.2 (38 %)	48.2 (35 %)
Entire year	24.2	147.1	139.5

4 Discussion

4.1 Partitioning the interannual variation in CO_2 exchange

The HOS model was used to partition the interannual variation (IAV) in CO_2 exchange into climatic variability and ecosystem functional change, which was reflected by the variability of the flux–climate relationship throughout the years (Hui et al., 2003). During the wet season, the daily NEE, GPP and RE were mainly related to T_a (Fig. 6). The effect of PAR on NEE and GPP was very weak, with R values of -0.05 and 0.08 , respectively.

A separate-slopes model was constructed for each year, and the multiple regression model was based on data from

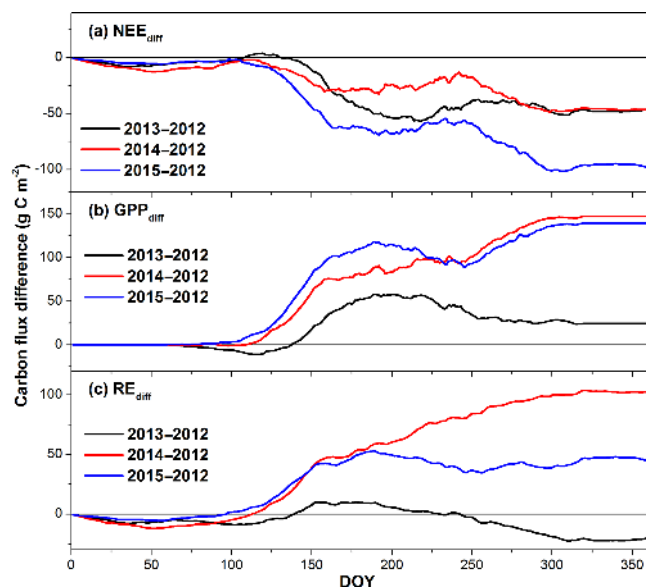
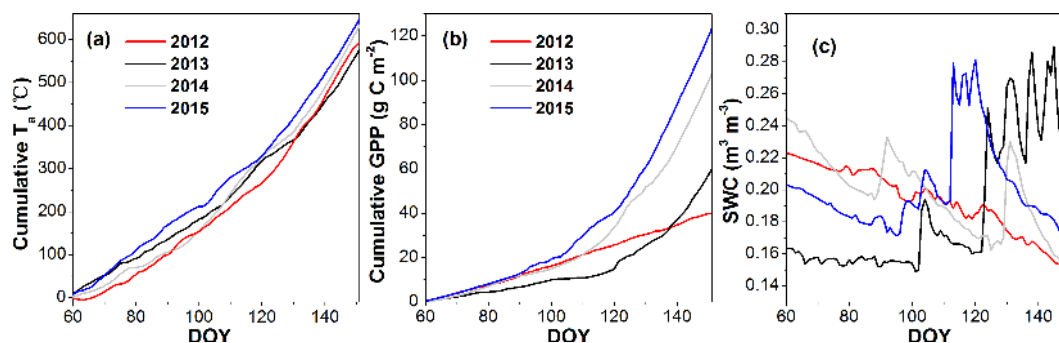


Figure 7. Seasonal variations in the differences of (a) NEE, (b) GPP and (c) RE from 2013 to 2012, from 2014 to 2012 and from 2015 to 2012.

the observational period. Compared with the multiple regression model, the separate-slopes model substantially improved the NEE estimation, with R^2 increasing from 0.69 in

Table 7. Comparison of mean annual temperature (MAT, °C), mean annual precipitation (MAP, mm yr⁻¹), NEE (g C m⁻² yr⁻¹), GPP, RE and RE / GPP between this study and previous grassland studies.

References/ Location	Ecosystem Description	Latitude	Longitude	Altitude	MAT	MAP	NEE	GPP	RE	RE / GPP
This study/ Lijiang, China	Alpine meadow/ shrub	27°10' N	100°14' E	3560	6.1	1180	-161 (-213 to -114)	600 (522 to 669)	444 (394 to 515)	0.74 (0.69 to 0.79)
Yu et al. (2006)/ Damxung, China	Alpine meadow	30°51' N	90°05' E	4250	2.1	520	28 (16 and 39)	167 (144 and 190)	195 (183 and 206)	1.16 (1.08 and 1.27)
Kato et al. (2006)/ Haibei, China	Alpine shrub	37°37' N	101°18' E	3250	-1.0	566	-121 (-193 to -79)	634 (575 to 681)	514 (489 to 556)	0.81 (0.72 to 0.86)
Shimoda et al. (2005)/ Japan	C3/C4 grassland	36°06' N	140°06' E	27	13.9	1156	-17 (-78 to 17)	2365 (2285 to 2426)	2348 (2303 to 2392)	0.99 (0.97 to 1.01)
Aires et al. (2008)/ Portugal	Mediterranean grassland	38°28' N	8°01' E	140	15.5	669	-71 (-190 and 49)	893 (524 and 1261)	822 (573 and 1071)	0.92 (0.85 and 1.09)
Jensen et al. (2017)/ Denmark	Meadow	55°55' N	8°24' E	0	8.7	809	-156 (-356 to -18)	1349 (1147 to 1570)	1193 (1069 to 1406)	0.88 (0.75 to 0.98)
Gilmanov et al. (2007)/ Europe	Multiple (19 sites)	-	-	-0.7 to 1770	3.9 to 14.6	387 to 1816	-150 (-653 to 171)	1261 (467 to 1874)	1111 (493 to 1622)	0.90 (0.59 to 1.14)
Xu and Baldocchi (2004)/ USA	Mediterranean grassland	38°24' N	120°57' E	129	16.3	559	-52 (-132 and 29)	798 (729 and 867)	747 (735 and 758)	0.94 (0.85 and 1.04)
Flanagan et al. (2002)/ Canada	Temperate grassland	49°26' N	112°34' E	951	-	378	-2 (-21 and 18)	280 (272 and 287)	278 (267 and 290)	1.0 (0.93 and 1.07)

**Figure 8.** Cumulative (a) T_a and (b) GPP and (c) the daily mean SWC from March to May (DOY60 to 151) for 2012, 2013, 2014 and 2015.

the multiple regression model to 0.79 in the separate-slopes model. This means that the separate-slopes model accounted for 10.3 % more variation in the observed NEE than the multiple regression model, which was attributed to the functional change (SS_f). The other 89.7 % of the variation in the observed NEE was partitioned to interannual climatic variability (SS_i , 7.7 %), seasonal climatic variation (SS_s , 37.7 %) and random error (SS_e , 44.3 %; Table 5). Therefore, most of the IAV in NEE, GPP and RE was attributable to the variation in climatic variables, in particular, climatic seasonal variation. This is in line with the findings reported for a Skjern meadow in Denmark and a temperate ombrotrophic bog in Canada (Jensen et al., 2017; Teklemariam et al., 2010). In contrast, Braswell et al. (1997) and Shao et al. (2014) found that functional change, rather than the direct effects of IAV in climate, accounted for more IAV in fluxes. Moreover, the contributions of different drivers to the IAV in GPP were similar to that of NEE, while the functional change in RE was twice that of NEE and GPP. The R^2 values for NEE, GPP and RE in the multiple regression model were 0.44, 0.53 and

0.59. It was considered reasonable that the largest random error was recorded for NEE.

4.2 Control of the interannual variation in the CO₂ exchange

To examine the interannual variation in CO₂ exchange, the cumulative NEE, GPP and RE in 2013, 2014 and 2015 were compared with the corresponding values in 2012 (Fig. 7). The cumulative NEE_{diff} (the difference in NEE) values for 2014–2012 and 2015–2012 increased rapidly in spring and autumn. In summer, the differences between 2012, 2014 and 2015 varied slightly. The cumulative NEE_{diff} for 2013–2012 increased from April to early August. These patterns were similar to those for GPP_{diff} . However, the annual cumulative GPP_{diff} (24.3 to 147.2 g C m⁻² yr⁻¹) was relatively larger than the annual cumulative NEE_{diff} (-44.2 to -98.3 g C m⁻² yr⁻¹). The cumulative RE_{diff} decreased from DOY 1 and then increased in spring. The cumulative RE_{diff} for 2013–2012 and 2015–2012 reached its maximum at the end of June, while the cumulative RE_{diff} for 2014–2012 in-

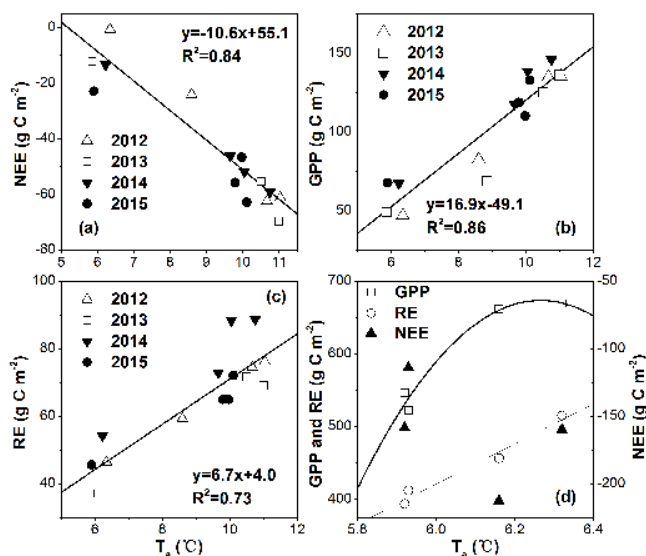


Figure 9. Relationships between (a) NEE and T_a ; (b) GPP and T_a ; (c) RE and T_s from July to October at a monthly scale and (d) relationship between the annual total CO₂ exchange fluxes and the mean annual T_a , which were $GPP = -1191T_a^2 + 14\,930T_a - 46\,102$, $R^2 = 0.97$ and $RE = 276T_a - 1235$, $R^2 = 0.97$.

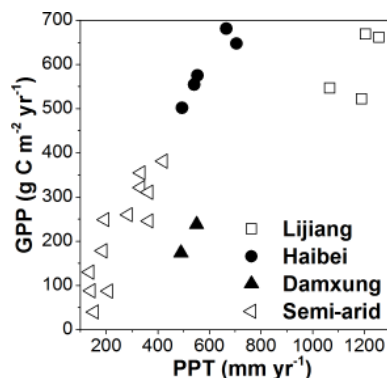


Figure 10. Relationships between the annual GPP and precipitation (PPT) for this Lijiang site, the Haibei site (Kato et al., 2006; Fu et al., 2009), the Damxung site (Fu et al., 2009) and the semi-arid grassland sites (Fu et al., 2009; Du and Liu, 2013; Yang and Zhou, 2013).

creased throughout the entire year and was the largest of all the periods considered.

The daily CO₂ uptake over this meadow ecosystem has previously been shown to increase with T_a (Wang et al., 2016). Especially in the spring (March to May), the temperature affected the vegetation growth and GPP. From March to May, the cumulative T_a was 592.3, 577.1, 633.1 and 647.6 °C in the 4 years from 2012 to 2015. Consequently, the cumulative GPP in the spring increased in the order of 2015 > 2014 > 2013. The exception was that the spring of 2012 had a higher T_a , but a lower GPP than the spring of 2013. Compared with the GPP in 2013, the GPP in 2012 in-

creased more significantly due to the higher T_a from March to April. However, the drought in May 2012 delayed vegetation growth and reduced GPP. The differences in GPP_{cum} for 2013–2012, 2014–2012 and 2015–2012 at the end of May were 20.0, 63.1 and 83.3 g C m⁻², representing 82.6, 42.9 and 59.7 % of the differences for the three periods.

From July to October, the NEE, GPP and RE were all strongly correlated with T_a on a monthly scale ($R^2 = 0.84$, 0.86 and 0.73; Fig. 9a, b, c). The slope of the relationship between GPP and T_a was much larger than for that between RE and T_a , indicating that when T_a increased, the alpine meadow ecosystem absorbed more CO₂. The monthly GPP in July and August varied slightly between the 4 years, while the interannual variability of the GPP in September was the largest because the monthly means T_a in September for 2012 (8.6 °C) and 2013 (8.8 °C) were significantly lower than those for 2014 (9.7 °C) and 2015 (10.0 °C). Consequently, the differences in GPP_{cum} for 2014–2012 and 2015–2012 from September to October were 55.2 and 48.2 g C m⁻², representing 37.5 and 34.6 % of the differences for the two periods.

On the annual scale, the annual total NEE decreased with the MAT in 2012, 2013 and 2015 and then increased when the MAT was highest in 2014. The reason for this was that the annual total RE increased linearly with the MAT ($R^2 = 0.97$), while the relationship between the GPP and MAT was non-linear (Fig. 9d). The GPP became saturated as the MAT increased. In contrast, the annual NEE increased with the MAT in the Haibei alpine meadow, which is in line with previous studies showing that the annual NEE is comprehensively controlled by the temperature environment (Kato et al., 2006).

4.3 Comparison of annual CO₂ exchange with other sites

The annual GPP at the study site was much larger than that reported in semi-arid grasslands in Tibet and Canada (Flanagan et al., 2002; Yu et al., 2006), but much lower than that reported in moist grasslands in low-lying areas in Europe (Table 7). In China, the annual GPP for semi-arid grasslands and the Haibei alpine meadow increased slightly with annual precipitation ($R^2 = 0.94$; Fig. 10). With similar annual precipitation, the annual GPP of the Damxung site was much lower than the Haibei site, possibly because of higher elevation. When the annual precipitation increased further, to over 1000 mm yr⁻¹, the annual GPP remained steady (Fig. 10). The annual GPP for the grassland ecosystems in China was always below 700 g C m⁻² yr⁻¹.

In addition to temperature effects, the daily RE was also correlated with the daily GPP ($RE = 0.44GPP + 0.63$, $R^2 = 0.82$) during the wet season from 2012 to 2015. Due to the high elevation and low soil temperature in the summer, the percentage of RE to GPP for this meadow site was lower than for Mediterranean grass-

lands ($RE = 0.53GPP + 0.72$, $R^2 = 0.85$, Aires et al., 2008; $RE = 0.47GPP + 1.33$, $R^2 = 0.85$, Xu and Baldocchi, 2004). The low level of RE resulted in a similar or even lower annual NEE (mean value: $-161 \text{ g C m}^{-2} \text{ yr}^{-1}$) at Lijiang than in moist grasslands with a low elevation (Table 7). For example, the mean annual NEE for a meadow in Denmark (annual precipitation: 809 mm) was $-156 \text{ g C m}^{-2} \text{ yr}^{-1}$, while the mean annual NEE for a C3/C4 grassland in Japan (annual precipitation: 1156 mm) was $-17 \text{ g C m}^{-2} \text{ yr}^{-1}$. The ratio of RE to GPP ranged from 0.69 to 0.79 over the Lijiang alpine meadow, which was lower than the Haibei alpine meadow (Table 7). This is why the annual NEE at the Lijiang site was on average 25 % lower than at the Haibei site. In general, low RE / GPP ratios occurred in high-altitude and moist areas. The alpine meadow ecosystem (Lijiang and Haibei) had a lower RE / GPP ratio than most low-lying grasslands. Compared with semi-arid grasslands (RE / GPP: approximately 1.0), the RE / GPP ratios reported in moist grasslands are much lower, e.g. a sown grassland in the Netherlands (0.60) and a natural grassland in Italy (0.59; Gilmanov et al., 2007).

5 Conclusions

The 4-year EC data from 2012 to 2015 were used to investigate the interannual variation in the NEE, GPP and RE. The key parameters for ecosystem photosynthesis and respiration were determined for the different seasons of each year. The vegetation growth (NDVI) controlled NEE_{sat} on a monthly scale, and the interannual variation in Q_{10} for the wet and dry seasons was small. The seasonal variation in CO_2 exchange was affected by the seasonal pattern of T_a and the soil moisture in the spring. In the spring, low T_a and drought events delayed the start time of CO_2 uptake. In the late wet season, the higher T_a in 2014 and 2015 resulted in later grass senescence and CO_2 release. The annual NEE decreased with the length of the CO_2 uptake period, but its relationship with the NDVI was not significant. For this alpine meadow, the HOS model suggests that most of the IAV in NEE, GPP and RE was attributed to the seasonal variation in climatic variables. On an annual scale, the annual RE increased linearly with the MAT, while the annual GPP became saturated when the MAT increased from 6.16 to 6.32 °C. Thus, the annual NEE decreased and then increased with the MAT. The low RE / GPP ratio at the study site was responsible for the lower annual NEE compared with some other grassland ecosystems with a larger GPP.

Data availability. Please contact the corresponding author to access data.

Competing interests. The authors declare that they have no conflict of interest.

Acknowledgements. This study was supported by the National Natural Science Foundation of China (grant no.: 91537212, 41675013, 41661144018, 41461144001, 41305012) and the Third Tibetan Plateau Scientific Experiment: Observations for Boundary Layer and Troposphere (GYHY201406001). The staffs from Lijiang Meteorological Administration are appreciated for their help in the maintenance of the measurements.

Edited by: J. Huang

Reviewed by: two anonymous referees

References

- Aires, L. M., Pio, C. A., and Pereira, J. S.: Carbon dioxide exchange above a Mediterranean C3/C4 grassland during two climatologically contrasting years, *Glob. Change Biol.*, 14, 539–555, 2008.
- Baldocchi, D.: “Breathing” of the terrestrial biosphere: lessons learned from aglobal network of carbon dioxide flux measurement systems, *Aust. J. Bot.*, 56, 1–26, 2008.
- Braswell, B. H., Schimel, D. S., Linder, E., and Moore, B.: The response of global terrestrial ecosystems to inter-annual temperature variability, *Science*, 278, 870–872, 1997.
- DAHV (Department of Animal Husbandry and Veterinary, Institute of Grasslands, Chinese Academy of Agricultural Sciences), and CISNR (Commission for Integrated Survey of Natural Resources, Chinese Academy of Sciences): Rangeland resources of China, China Agricultural Science and Technology, Beijing, 1996.
- Du, Q. and Liu, H. Z.: Seven years of carbon dioxide exchange over a degraded grassland and a cropland with maize ecosystems in a semiarid area of China, *Agr. Ecosyst. Environ.*, 173, 1–12, 2013.
- Falge, E., Baldocchi, D., and Olson, R.: Gap filling strategies for defensible annual sums of net ecosystem exchange, *Agr. Forest Meteorol.*, 107, 43–69, 2001.
- Fan, Z. X., Bräuning, A., Thomas, A., Li, J. B., and Cao, K. F.: Spatial and temporal temperature trends on the Yunnan Plateau (Southwest China) during 1961–2004, *Int. J. Climatol.*, 31, 2078–2090, 2011.
- Flanagan, L., Wever, L. A., and Carlson, P.: Seasonal and interannual variation in carbon dioxide exchange and carbon balance in a northern temperate grassland, *Glob. Change Biol.*, 8, 599–615, 2002.
- Foken, T. and Wichura, B.: Tools for quality assessment of surface-based flux measurements, *Agr. Forest Meteorol.*, 78, 83–105, 1996.
- Fu, Y., Zheng, Z., Yu, G., Hu, Z., Sun, X., Shi, P., Wang, Y., and Zhao, X.: Environmental influences on carbon dioxide fluxes over three grassland ecosystems in China, *Biogeosciences*, 6, 2879–2893, doi:10.5194/bg-6-2879-2009, 2009.
- Gilmanov, T. G., Soussana, G. F., Aires, L., Allard, V., Ammann, C., Balzarolo, M., Barcza, Z., Bernhofer, C., Campbell, C. L., and Cernusca, A.: Partitioning European grassland net ecosystem CO_2 exchange into gross primary productivity and ecosystem respiration using light response function analysis, *Agr. Ecosyst. Environ.*, 121, 93–120, 2007.
- Gilmanov, T. G., Aires, L., Barcza, Z., Baron, V. S., Belelli, L., Beringer, J., Billesbach, D., Bonal, D., Bradford, J., Ceschia, E., Cook, D., Corradi, C., Frank, A., Gianelle, D., Gimeno, C.,

- Grünwald, T., Guo, H., Hanan, N., Haszpra, L., Heilman, J., Jacobs, A., Jones, M. B., Johnson, D. A., Kiely, G., Li, S., Magliulo, V., Moors, E., Nagy, Z., Nasyrov, M., Owensby, C., Pinter, K., Pio, C., Reichstein, M., Sanz, M. J., Scott, R., Soussana, J. F., Stoy, P. C., Svejcar, T., Tuba, Z., and Zhou, G.: Productivity, respiration, and light-response parameters of world grassland and agroecosystems derived from flux-tower measurements, *Rangel. Ecol. Manage.*, 63, 16–39, 2010.
- Gu, S., Tang, Y. H., Du, M. Y., Kato, T., Li, Y. N., Cui, X. Y., and Zhao, X. Q.: Short term variation of NEE in relation to environmental controls in an alpine meadow on the Qinghai-Tibetan Plateau, *J. Geophys. Res.*, 108, doi:10.1029/2003JD003584, 2003.
- Guo, L. N., He, Z. J., Long, X., Wang, J. Z., Wang, L. D., and Li, C. X.: Soil characteristics and its classification system in Mt. Yulong, China, *Guangxi, Agr. Sci.*, 40, 1177–1183, 2009 (in Chinese).
- Huang, J., Zhang, W., Zuo, J., Bi, J., Shi, J., Wang, X., Chang, Z., Huang, Z., Yang, S., Zhang, B., Wang, G., Feng, G., Yuan, J., Zhang, L., Zuo, H., Wang, S., Fu, C., and Chou, J.: An overview of the semi-arid climate and environment research observatory over the Loess Plateau, *Adv. Atmos. Sci.*, 25, 906–921, 2008.
- Huang, J., Yu, H., Guan, X., Wang, G., and Guo, R.: Accelerated dryland expansion under climate change, *Nat. Clim. Change*, 6, 166–171, 2016.
- Hui, D., Luo, Y., and Katul, G.: Partitioning interannual variability in net ecosystem exchange between climatic variability and functional change, *Tree Physiol.*, 23, 433–442, 2003.
- Hunt, J. E., Kelliher, F. M., Mcseveny, T. M., Ross, D. J., and Whitehead, D.: Long-term carbon exchange in a sparse, seasonally dry tussock grassland, *Glob. Change Biol.*, 10, 1785–1800, 2004.
- Jensen, R., Herbst, M., and Friberg, T.: Direct and indirect controls of the interannual variability in atmospheric CO₂ exchange of three contrasting ecosystems in Denmark, *Agr. Forest Meteorol.*, 233, 12–31, 2017.
- Jing, X., Huang, J., Wang, G., Higuchi, K., Bi, J., Sun, Y., Yu, H., and Wang, T.: The effects of clouds and aerosols on net ecosystem CO₂ exchange over semi-arid Loess Plateau of Northwest China, *Atmos. Chem. Phys.*, 10, 8205–8218, doi:10.5194/acp-10-8205-2010, 2010.
- Kato, T., Tang, Y. H., Gu, S., Cui, X. Y., Hirota, M., Du, M. Y., Li, Y. N., Zhao, X. Q., and Oikawa, T.: Seasonal patterns of gross primary production and ecosystem respiration in an alpine meadow ecosystem on the Qinghai-Tibetan Plateau, *J. Geophys. Res.*, 109, 1045–1056, doi:10.1029/2003JD003951, 2004.
- Kato, T., Tang, Y. H., Gu, S., Hirota, M., Du, M. Y., Li, Y. N., and Zhao, X. Q.: Temperature and biomass influences on interannual changes in CO₂ exchange in an alpine meadow on the Qinghai-Tibetan Plateau, *Glob. Change Biol.*, 12, 1285–1298, 2006.
- Kormann, R. and Meixner, F. X.: An analytical footprint model for nonneutral stratification, *Bound.-Layer Meteorol.*, 99, 207–224, 2001.
- Liu, J., Zhang, Y., Li, Y., Wang, D., Han, G., and Hou, F.: Overview of grassland and its development in China. Multifunctional grasslands in a changing world volume (I), Guangdong People's Publishing House, Guangzhou, 3–5, 2008.
- Liu, X. D. and Chen, B. D.: Climatic warming in the Tibetan Plateau during recent decades, *Int. J. Climatol.*, 20, 1729–1742, 2000.
- Lloyd, J. and Taylor, J. A.: On the temperature-dependence of soil respiration, *Funct. Ecol.*, 8, 315–323, 1994.
- Moore, C. J.: Frequency response corrections for eddy correlation systems, *Bound.-Lay. Meteorol.*, 37, 17–35, 1986.
- Parton, W. J., Scurlock, J. M. O., Ojima, D. S., Schimel, D. S., and Hall, D. O.: Impact of climate change on grassland production and soil carbon worldwide, *Glob. Change Biol.*, 1, 13–22, 1995.
- Polley, H. W., Frank, A. B., Sanabria J., and Phillips, R.: Interannual variability in carbon dioxide fluxes and flux-climate relationships on grazed and ungrazed northern mixed-grass prairie, *Glob. Change Biol.*, 14, 1620–1632, 2008.
- Richardson, A. D., Hollinger, D. Y., Aber, J. D., Ollinger, S. V., and Braswell, B. H.: Environmental variation is directly responsible for short- but not long-term variation in forest atmosphere carbon exchange, *Global. Change Biol.*, 13, 788–803, 2007.
- Shao, J., Zhou, X., He, H., Yu, G., Wang, H., Luo, Y., Chen, J., Gu, L., and Bo, L.: Partitioning climatic and biotic effects on interannual variability of ecosystem carbon exchange in three ecosystems, *Ecosystems*, 17, 1186–1201, 2014.
- Shi, P. L., Sun, X. M., and Xu, L. L.: Net ecosystem CO₂ exchange and controlling factors in a steppe-Kobresia meadow on the Tibetan Plateau, *Sci. China-Earth Sci.*, 49, 207–218, 2006.
- Shimoda, S., Mo, W., and Oikawa, T.: The effects of characteristics of Asian monsoon climate on interannual CO₂ exchange in a humid temperate C3/C4 co-occurred grassland, *SOLA*, 1, 169–172, 2005.
- Suyker, A. E., Verma, S. B., and Burba, G. G.: Interannual variability in net CO₂ exchange of a native tallgrass prairie, *Glob. Change Biol.*, 5, 255–265, 2003.
- Teklemariam, T. A., Lafleur, P. M., Moore, T. R., Roulet, N. T., and Humphreys, E. R.: The direct and indirect effects of inter-annual meteorological variability on ecosystem carbon dioxide exchange at a temperate ombrotrophic bog, *Agr. Forest Meteorol.*, 150, 1402–1411, 2010.
- Vickers, D. and Mahrt, L.: Quality control and flux sampling problems for tower and aircraft data, *J. Atmos. Ocean. Technol.*, 14, 512–526, 1997.
- Wang, L., Liu, H. Z., and Bernhofer, C.: Response of carbon dioxide exchange to grazing intensity over typical steppes in a semi-arid area of Inner Mongolia, *Theor. Appl. Climatol.*, 127, 1–12, doi:10.1007/s00704-016-1736-7, 2016a.
- Wang, L., Liu, H. Z., Sun, J. H., and Feng, J. W.: Water and carbon dioxide fluxes over an alpine meadow in southwest China and the impact of a spring drought event, *Int. J. Biometeorol.*, 60, 195–205, 2016b.
- Webb, E. K., Pearman, G. I., and Leuning, R.: Correction of flux measurements for density effects due to heat and water vapour transfer, *Q. J. R. Environ. Soc.*, 106, 85–100, 1980.
- Wilczak, J. M., Oncley, S. P., and Stage, S. A.: Sonic anemometer tilt correction algorithms, *Bound.-Lay. Meteorol.*, 99, 127–150, 2001.
- Xu, L. K. and Baldocchi, D.: Seasonal variation in carbon dioxide exchange over a Mediterranean annual grassland in California, *Agr. Forest Meteorol.*, 1232, 79–96, 2004.
- Yang, F. L. and Zhou, G. S.: Sensitivity of temperate desert steppe carbon exchange to seasonal droughts and precipitation variations in Inner Mongolia, China, *PLoS One*, 8, e55418, doi:10.1371/journal.pone.0055418, 2013

Yu, G. R., Fu, Y., Sun, X., Wen, X., and Zhang, L.: Recent progress and future directions of ChinaFLUX, *Sci. China-Earth Sci.*, 49, 1–23, 2006.

Zhao, L., Li, Y., Xu, S. Y., Zhou, H. K., Gu, S., Yu, G. R., and Zhao, X. Q.: Diurnal, seasonal and annual variation in net ecosystem CO₂ exchange of an alpine shrubland on Qinghai-Tibetan plateau, *Glob. Change Biol.*, 12, 1940–195, 2006.